ELSEVIER

Journal of Power Sources 109 (2002) 281–286

JOURNAL OF POWER SOURCES

www.elsevier.com/locate/jpowsour

Microelectrochemistry study of metal-hydride battery materials Cycling behavior of $LaNi_{3.55}Mn_{0.4}Al_{0.3}Co_{0.75}$ compared with $LaNi_5$ and its mono-substituted derivatives

A. Merzouki[a], C. Cachet-Vivier[b,*], V. Vivier[b], J.-Y. Nédélec[b], L.T. Yu[b], N. Haddaoui[a], J.-M. Joubert[c], A. Percheron-Guégan[c]

[a]*Laboratoire de Physico-Chimie des Hauts Polymères, Dépt. Génie des Procédés, Faculté des Sciences de l'Ingénieur, Université F. Abbas, Sétif 19000, Algeria*

[b]*Laboratoire d'Electrochimie Catalyse et Synthèse Organique -UMR 7582 CNRS-Université Paris 12, 2-8 rue H. Dunant, 94320 Thiais, France*

[c]*Laboratoire de Chimie Métallurgique des Terres Rares, CNRS, 2-8 rue H. Dunant, 94320 Thiais, France*

Received 9 November 2001; received in revised form 18 January 2002; accepted 22 January 2002

Abstract

$LaNi_5$ intermetallic-hydride forming compound and several metal-substituted derivatives have been compared in terms of cycling behavior observed by means of the cavity microelectrode (CME) at high scan rates (50 mV s^{-1}). $LaNi_{3.55}Mn_{0.4}Al_{0.3}Co_{0.75}$ was found to have a stable behavior over 1000 cycles, whereas, the capacity of $LaNi_5$ decreases after only 200 cycles. The performances for the mono-substituted compounds are intermediate. The rechargeability decreases according to the following order: $LaNi_{4.6}Mn_{0.4} > LaNi_{4.7}Al_{0.3} > LaNi_{4.25}Co_{0.75} > LaNi_5$. This study demonstrates the capability of the CME to check numerous battery materials in a very short period of time, which allows to bring out the effect due to the corrosion of the material.

Keywords: Mono-substituted; Intermetallic compounds; Cavity microelectrode

1. Introduction

$LaNi_5$ intermetallic compound and its metal-substituted derivatives are studied by numerous authors, because they are used in nickel–metal-hydride (Ni–MH) batteries as anodic material, replacing the toxic Cd element in alkaline batteries. Binary $LaNi_5$ suffers from severe corrosion during cycling due to the intermetallic decomposition in the alkaline electrolyte, resulting in a fast decrease of the capacity as a function of cycle number [1]. To overcome this problem, various substituted derivatives have been studied leading to the set-up of a composition [$MmNi_{3.55}Mn_{0.4}Al_{0.3}Co_{0.75}$ (Mm: mischmetal)] offering adequate compromise between initial capacity and cycle life [2,3]. These compounds are usually studied with the composite electrode device. However, the size of such an electrode (1 cm in diameter and a fraction of a mm in thickness) induces both high ohmic drop and double layer capacitance, which distort voltammograms. For minimizing these side phenomena, low potential scan rates (lower than 1 mV s^{-1}) must be used. The cavity microelectrode (CME) [4–9], also called the powder electrode, which is recently developed, presents dimensions of 50 μm diameter and 20 μm depth. It allows the study of pure materials using scan rates higher than some tens of mV s^{-1}. Accordingly, it is possible to achieve several hundred cycles within a short time. In the present work, we compare the cyclability of the three-substituted $LaNi_{3.55}Mn_{0.4}Al_{0.3}Co_{0.75}$ compound with one of the binary $LaNi_5$ and single-substituted $LaNi_{5-x}M_x$ (M = Mn, Al, Co) compounds in order to check the possibility of evaluating the cycling behavior of metal-hydride electrodes with the short term cycling procedure given by the CME method.

2. Experimental

The materials are synthesized by induction melting of the elements followed by an appropriate annealing treatment. Homogeneity and single phase character is checked by X-ray diffraction and electron probe microanalysis [10]. The materials were manually ground in a mortar and SEM

* Corresponding author. Tel.: +33-149-7811-37; fax: +33-149-7811-48.
E-mail address: cachet@glvt-cnrs.fr (C. Cachet-Vivier).

0378-7753/02/$ – see front matter
PII: S0378-7753(02)00074-5

photographs reveal a non-homogeneous grain-size distribution and irregular shapes. The size of the biggest grains was in the range 30–50 μm and that of the smallest ones was inferior to a few μm.

Electrochemical experiments were performed in a classical three-electrode cell using an AUTOLAB PT30 potentiostat (Ecochemie). The working electrode is a CME which has been previously described [7–9]. The cavity is filled up with material grains using the electrode as a pestle. After electrochemical measurements, we ensure that the material is still present within the cavity. Then the cavity is unloaded by washing it in a 1 mol l^{-1} HCl solution. Concurrent use of an ultrasonic treatment favors the dissolution of the material. We insure that the cavity is particle-free after washing by observing it with a microscope (Olympus BX30) equipped with a numerical camera unit (Olympus DP10). The reference electrode is an Hg/HgO electrode filled with a 7 M KOH solution and the counter electrode is a stainless steel wire in a separated compartment. KOH solution is deoxygenated by bubbling with Ar gas. As the material is a good electronic conductor, the adjunction of graphite or carbon black is never done.

3. Results and discussion

Fig. 1a shows the first, the second and the twentieth cycle recorded at 10 mV s^{-1} for $LaNi_{3.55}Mn_{0.4}Al_{0.3}Co_{0.75}$. From the first cycle, and all the successive cycles, one observes a shoulder on the water reduction wall and a wide anodic peak located at about −0.8 V/Hg/HgO. This curve shape is typical of the various studied samples. About 20 conditioning cycles are necessary for obtaining a stable curve except for $LaNi_{4.7}Al_{0.3}$ which needs 100 cycles. After stabilization of the curves, the samples are submitted to increasing scan rates from 5 to 500 or 1000 mV s^{-1}, after which a last scan at 50 mV s^{-1} is carried out. A slight charge increase of a few percent is observed between this last scan and the one previously obtained at 50 mV s^{-1}, which represents some tens of cycles. This slight increase is likely due to a complex process, such as local cleavage of the largest grains, which increases and improves the contact between the grains. The voltammograms recorded at 50 mV s^{-1} are also similar to those recorded from the second cycle at 10 mV s^{-1}, which is exemplified by the voltammogram drawn in Fig. 1b.

The curve drawn in dashed line corresponds to an empty cavity, which explains the electrochemical behavior of the platinum collector in 7 M KOH. Thus, the curve obtained when the material is present in the cavity can not be due to the oxidation of H_2 or H adsorbed on the platinum collector. The performance of the compound as a battery material can be described through the variation of the anodic peak area, which corresponds to a direct evaluation of the available charge Q_A during the discharge stage. The peak characteristics, i.e. peak area A_A and peak intensity I_A, are determined from the baseline drawn in dotted line on Fig. 1b by interpolating the capacitive anodic current. Q_A is calculated through the relationship:

$$Q_A = \frac{A_A}{v} \quad (1)$$

where v is the scan rate.

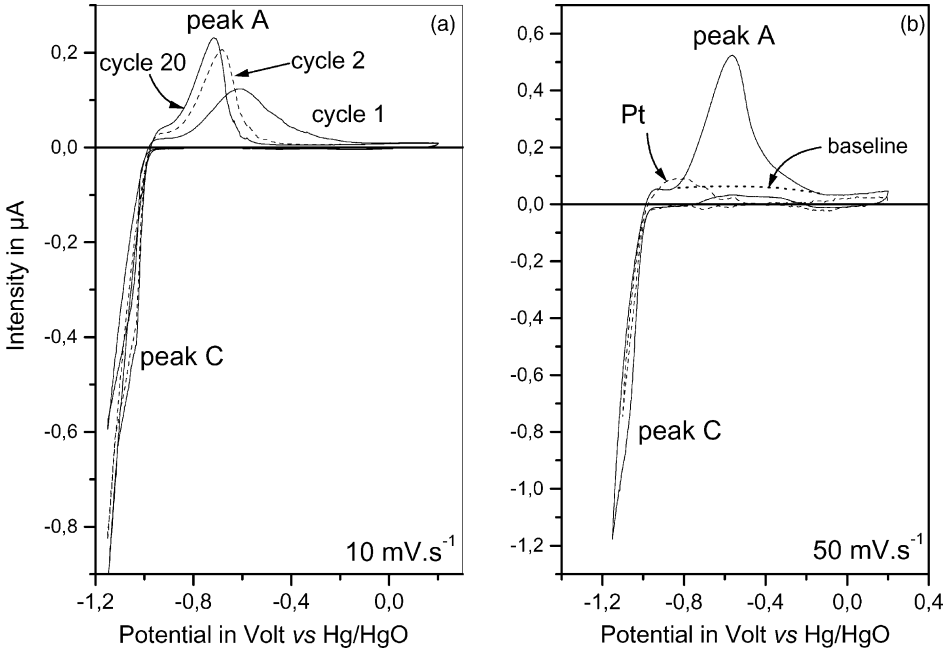

Fig. 1. (a) Voltammograms recorded at 10 mV s^{-1} on $LaNi_{3.55}Mn_{0.4}Al_{0.3}Co_{0.75}$ at cycles 1, 2 and 20; (b) voltammograms recorded at 50 mV s^{-1} of $LaNi_{3.55}Mn_{0.4}Al_{0.3}Co_{0.75}$ after scan rate study (full line) and of the platinum collector (dashed line). The baseline used for the peak integration is drawn as dotted line.

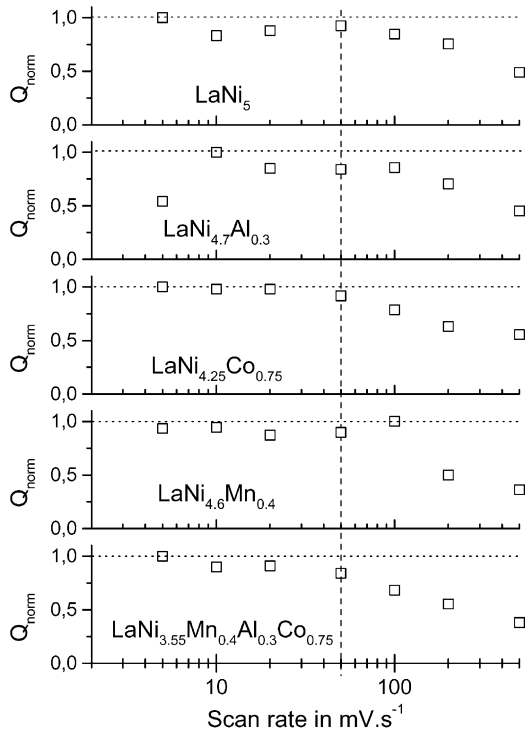

Fig. 2. Evolution of the normalized exchanged charge $Q_{norm} = Q_A/Q_A^{max}$ vs. the scan rate, v.

Fig. 2 shows the variation of the normalized charge Q_{norm} versus the scan rate v. Q_{norm} is defined as

$$Q_{norm} = \frac{Q_A}{Q_A^{max}}, \quad (2)$$

where Q_A^{max} is the maximum value of Q_A reached during the scan rate variation and is specific for each sample. We can consider that the exchanged charge remains constant for scan rates lower than 50 or 100 mV s^{-1}. This leads to the conclusion that all the electroactive sites in the material are implicated in the electrochemical reaction within this scan rate range. For scan rates higher than 100 mV s^{-1}, Q_{norm} strongly decreases for all compounds. As a result, the cycling performance tests for these intermetallic compounds have to be done with a scan rate lower than 100 mV s^{-1}.

The graphs in Fig. 3 are related to voltammograms recorded at 50 mV s^{-1} during 1000 cycles, for $LaNi_5$, $LaNi_{4.7}Al_{0.3}$, $LaNi_{4.25}Co_{0.75}$, $LaNi_{4.6}Mn_{0.4}$, and $LaNi_{3.55}Mn_{0.4}Al_{0.3}Co_{0.75}$, respectively. For several compounds, curve stabilization needs more than 20 cycles, i.e. more than needed at lower scan rates. It appears that Mn endows a stability of the potential and of the peak shape while Al brings stability of the intensity. We note that $LaNi_5$, the unsubstituted sample, shows the more erratic evolution of the curve shape, while the tri-substituted sample, $LaNi_{3.55}Mn_{0.4}Al_{0.3}Co_{0.75}$ shows the smallest change of the curve shape; it has the potential stability of the Mn-substituted compound and the intensity stability of the Al-substituted one.

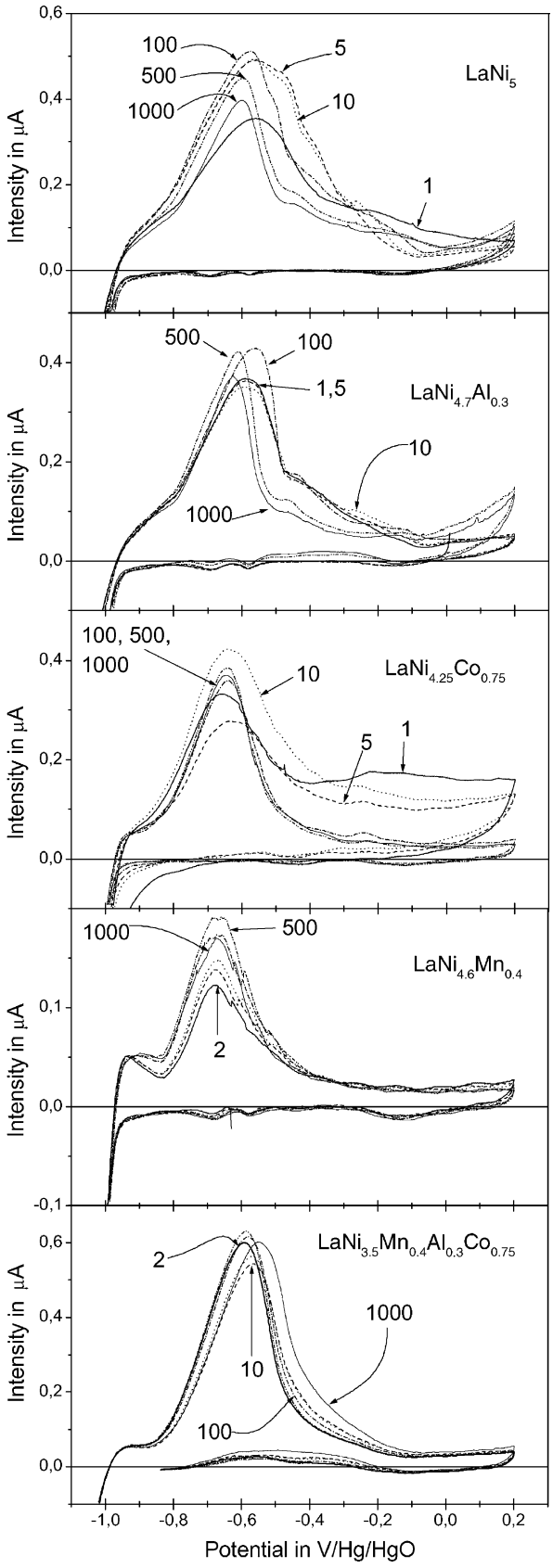

Fig. 3. Voltammograms recorded at 50 mV s^{-1} on $LaNi_5$, $LaNi_{4.7}Al_{0.3}$, $LaNi_{4.25}Co_{0.75}$, $LaNi_{4.6}Mn_{0.4}$, and $LaNi_{3.55}Mn_{0.4}Al_{0.3}Co_{0.75}$ for different cycle numbers.

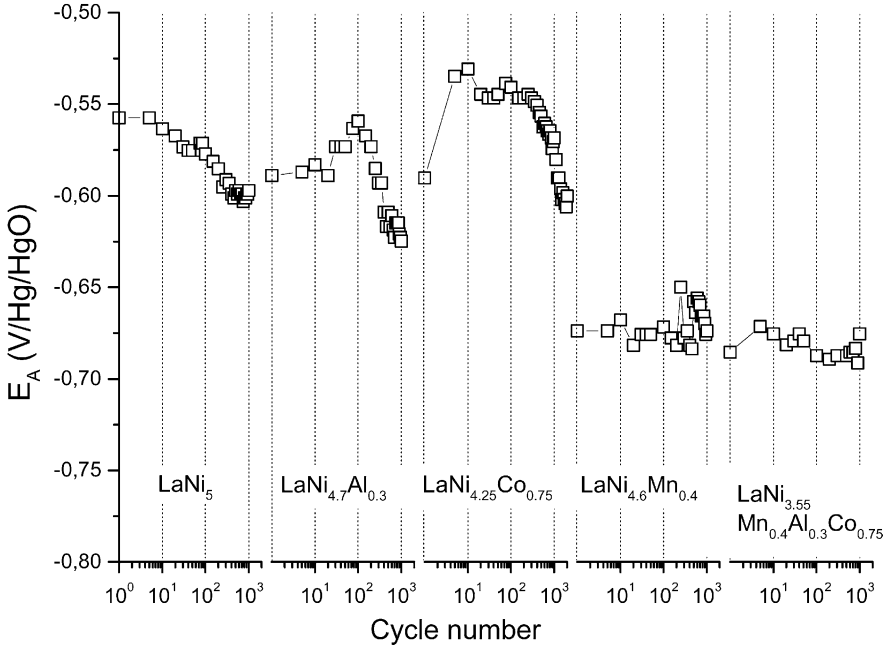

Fig. 4. Variation of the peak potential (E_A) vs. the number of cycles for $LaNi_5$, $LaNi_{4.7}Al_{0.3}$, $LaNi_{4.25}Co_{0.75}$, $LaNi_{4.6}Mn_{0.4}$, and $LaNi_{3.55}Mn_{0.4}Al_{0.3}Co_{0.75}$.

From these measurements, we can plot the peak potential E_A (Fig. 4), and the normalized peak intensity I_{norm} defined by the ratio between the peak intensity I_A and the maximum peak intensity I_A^{max} reached during cycling (Fig. 5) versus the cycle number. The following can be noted:

(i) For $LaNi_{4.6}Mn_{0.4}$ and $LaNi_{3.55}Mn_{0.4}Al_{0.3}Co_{0.75}$, the overall peak potential is lowered during cycling, which can be attributed to the presence of Mn (Fig. 4). Moreover, the variation amplitude of E_A is about 40 mV when Mn is present. This variation is smaller than for the other elements, for which it can reach about 75 mV.
(ii) For all the samples, the peak intensity increases during the first hundred cycles and stays more or less stable, then decreases except for the three-substituted sample.

Fig. 6 shows the variation of the normalized charge Q_{norm} versus cycle number, Q_{norm} being defined in Eq. (2), where Q_A^{max} is, in the present case, the maximum value of Q_A during cycling. The following can be noted:

(i) For all the samples, the capacity increases more or less during the first 100 cycles. This can result from a cleavage of the largest grains due to the specific volume difference between the hydrogenated material and the non-hydrogenated one from 10% for $LaNi_{3.55}Mn_{0.4}Al_{0.3}Co_{0.75}$ to 22.4% for $LaNi_5$ [10]. This activation procedure corresponds to an increase of the electrochemical interface between the grains and to a modification of surface properties [11]. However, these cleavages corresponding to grain-size reduction do not seem to hinder electrical contacts between grains in the electrode.

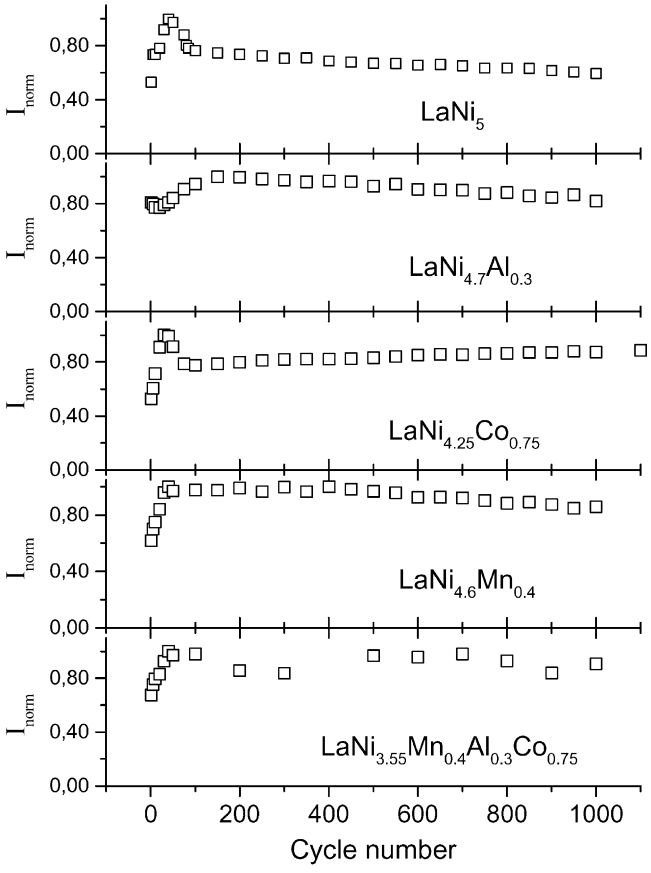

Fig. 5. Variation of the normalized intensity I_{norm} vs. the number of cycles for $LaNi_5$, $LaNi_{4.7}Al_{0.3}$, $LaNi_{4.25}Co_{0.75}$, $LaNi_{4.6}Mn_{0.4}$, and $LaNi_{3.55}Mn_{0.4}Al_{0.3}Co_{0.75}$.

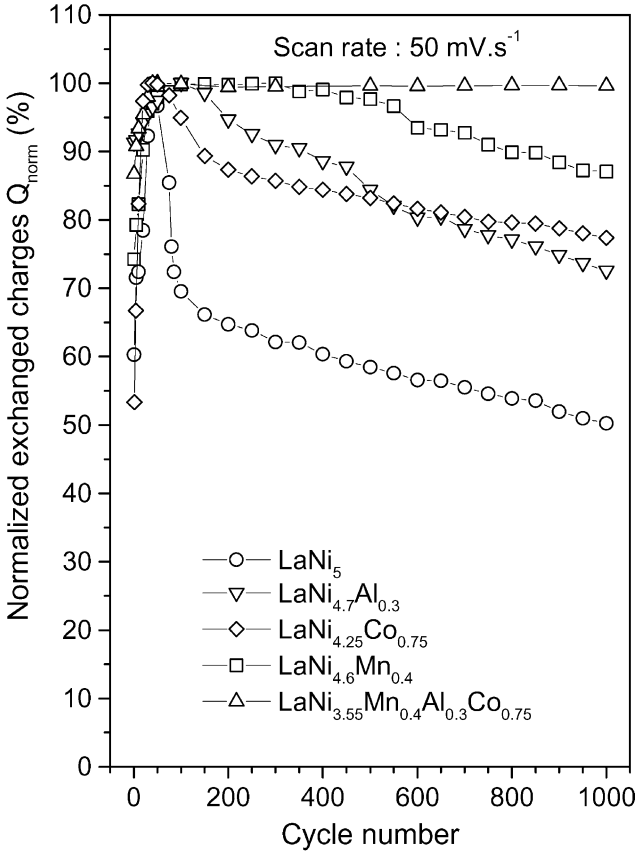

Fig. 6. Comparison of the variation of the normalized charge Q_{norm} vs. the number of cycles.

(ii) The capacity rapidly decreases for $LaNi_5$ and slowly for the mono-substituted derivatives. After 1000 cycles, it reaches 50 and 80–90% of the maximum capacity, respectively. Only the capacity of the three-substituted sample, $LaNi_{3.55}Mn_{0.4}Al_{0.3}Co_{0.75}$, remains constant over 1000 cycles. These results globally enhance those obtained through an intensiostatic method with a composite electrode for which the cycle number reaches a few hundred cycles [11]. It should be noted that, the cycling tests over 1000 cycles are performed in less than one day with the CME at 50 mV s^{-1}, whereas, it needs nearly one year at only 0.1 mV s^{-1}.

However, it appears that the substitution of Ni in $LaNi_5$ by various metals improves the cycle life in the order Mn > Al > Co. This order is surprising regarding Sakai et al. [12], as well as, Baddour-Hadjean et al. [13]. They found that Mn was the least effective metal for improving corrosion resistance. Cycling tests realized by Baddour-Hadjean et al. [13] showed that the Co-substituted alloy had the best stability, whereas, the Al-substituted one exhibits a rather high sensitivity to corrosion. Furthermore, it was shown by other authors that increasing amounts of Al and Co improve stability [14,15]. Corrosion inhibition due to these metals has been attributed to a surface effect, like the formation of protective surface oxides [15,16]. However, it was shown later that Al corrosion products dissolve in KOH [17]. Moreover, Adzic et al. [18] have shown that Co-free electrodes rapidly corrode. Thus, it is possible that this passivation layer of Co oxides cannot be formed fast enough when cyclings are performed at high scan rates with the CME. On the contrary, Mn would be rapidly oxidized and then prevent Ni corrosion. This hypothesis can be argued by the examination of the potential pH diagrams [19,20]. They show that Mn and Al metals are thermodynamically very unstable and should rapidly react to produce H_2 and the corresponding oxide and/or dissolved species. The micro-cavity represents a confined volume and it is probably saturated with dissolved species which precipitate in the oxide form at the beginning of the cycling tests, acting as a protective layer. However, the capacity of $LaNi_{4.6}Mn_{0.4}$ and $LaNi_{4.7}Al_{0.3}$ progressively decrease due to a progressive dissolution of the Mn and Al oxides; this one is more rapid for Al according to the respective solubilities 10^{-4} and 1 mol l^{-1}.

Two additional effects could explain the discrepancies obtained with regard to the cycling behavior between the CME method and the composite electrode methods. First, we have to compare data obtained by voltammetric measurements to intentiostatic measurements. Secondly, the difference of time scale between the two experiments is of the order 1:100. We believe that the measurements with the CME are not affected by the so-called calendar corrosion due to the time of immersion in the electrolyte, which is added to the corrosion due to the effect of cycling in the usual tests on composite electrodes. This corrosion type has been shown by Maurel et al. [21], to be the main factor since corrosion products are the same for cycled or non-cycled electrodes immersed for the same time in KOH. While explaining the differences between the relative order found in our work compared with literature data, this phenomenon also explains why larger cycle lives are obtained for all the compounds compared to the macroelectrode studies. This result gives additional support to the conclusion that, calendar corrosion is the main factor affecting cycle life of the electrodes.

4. Conclusion

Cycle life tests have been performed with the CME method on several hydride forming materials. The best results have been obtained for the three-substituted $LaNi_{3.55}Mn_{0.4}Al_{0.3}Co_{0.75}$ compound, the worst for the binary $LaNi_5$. This behavior is the same as observed for usual composite electrodes. This shows the outstanding ability of the CME method to perform cyclability tests within times as short as one day, while the usual tests last several months. Moreover, the possible deconvolution of the calendar corrosion from the purely cycling-due-to-corrosion opens future

developments for the understanding of the metal-hydride electrode behavior and for the design of new materials with improved cycle life.

References

[1] J.J.G. Willems, Philips J. Res. Suppl. 39 (1984) 1.
[2] M. Ikoma, H. Kawano, I. Matsumoto, N. Yanagihara, Eur. Patent Appl. 0,271,043 (1987).
[3] H. Ogawa, M. Ikoma, H. Kawano, I. Matsumoto, J. Power Sources 12 (1988) 393.
[4] H.X. Yang, C.S. Cha, J. Power Sources 43 (1993) 145.
[5] C.S. Cha, C.M. Li, H.X. Yang, P.F. Liu, J. Electroanal. Chem. 368 (1994) 47.
[6] W. Yang, G. Zhang, S. Lu, J. Xie, Q. Liu, Solid State Ionics 121 (1999) 85.
[7] V. Vivier, C. Cachet-Vivier, B.L. Wu, C.S. Cha, J.-Y. Nedelec, L.T. Yu, Electrochem. Solid State Lett. 2 (1999) 385.
[8] V. Vivier, C. Cachet-Vivier, C.S. Cha, J.-Y. Nedelec, L.T. Yu, Electrochem. Commun. 2 (2000) 180.
[9] V. Vivier, C. Cachet-Vivier, S. Mezaille, B.L. Wu, C.S. Cha, J.-Y. Nedelec, M. Fedoroff, D. Michel, L.T. Yu, J. Electrochem. Soc. 147 (2000) 4252.
[10] J.-M. Joubert, M. Latroche, R. Cerný, A. Percheron-Guégan, K. Yvon, J. Alloys Comp., in press.
[11] J.J. Reilly, G.D. Adzic, J.R. Johnson, T. Vogt, S. Mukerjee, J. McBreen, J. Alloys Comp. 293–295 (1999) 569.
[12] T. Sakai, K. Oguro, H. Miyamura, H. Kuriyama, A. Kato, H. Ishikawa, J. Less Common Met. 161 (1990) 193.
[13] R. Baddour-Hadjean, J.-P. Pereira-Ramos, M. Latroche, A. Percheron-Guégan, ITE letters on batteries, New Technol. Med. 1 (2000) 29.
[14] M. Kanda, M. Yamamoto, K. Kanno, Y. Satoh, H. Hayashida, M. Suzuki, J. Less Common Met. 129 (1987) 13.
[15] S. Mukerjee, J. McBreen, G.D. Adzic, J.R. Johnson, J.J. Reilly, Extended Abstracts, National Meeting of the Electrochemical Society, San Antonio, TX, USA, October, Vol. 96 (2) (1996).
[16] T. Sakai, H. Miyamura, H. Kuriyama, A. Kato, K. Oguro, H. Ishikawa, J. Less Common Met. 159 (1990) 127.
[17] P. Leblanc, C. Jordy, B. Knosp, P. Blanchard, J. Electrochem. Soc. 145 (1998) 860.
[18] G. Adzic, J.R. Johnson, S. Mukerjee, J. McBreen, J.J. Reilly, J. Alloys Comp. 231 (1995) 537.
[19] M. Pourbaix, Atlas d'équilibres électrochimiques, Gauthier-Villars & Cie Editeurs, Paris, 1963.
[20] H. Senoh, M. Ueda, N. Furukawa, H. Inoue, C. Iwakura, J. Alloys Comp. 280 (1998) 114.
[21] F. Maurel, B. Knosp, M. Backhaus-Ricoult, J. Electrochem. Soc. 147 (1) (2000) 78.